Design of the sample cell in near-field surface-enhanced Raman scattering by finite difference time domain method

Yaqin Li (李亚琴), Guoshu Jian (简国树), and Shifa Wu (吴世法)

Department of Physics, Dalian University of Technology, Dalian 116024

Received June 5, 2006

The rational design of the sample cell may improve the sensitivity of surface-enhanced Raman scattering (SERS) detection in a high degree. Finite difference time domain (FDTD) simulations of the configuration of Ag film-Ag particles illuminated by plane wave and evanescent wave are performed to provide physical insight for design of the sample cell. Numerical solutions indicate that the sample cell can provide more "hot spots" and the massive field intensity enhancement occurs in these "hot spots". More information on the nanometer character of the sample can be got because of gradient-field Raman (GFR) of evanescent wave.

OCIS codes: 290.5860, 240.0310, 240.6680, 999.9999 (surface-enhanced Raman scattering).

The surface enhanced Raman scattering (SERS)[1] is based on plasmon resonances to produce massive amplifications of the local field and boost the intensity of the essentially weak Raman scattering process. The largest SERS signals are believed to come from the "hot spots", spatially in which the electric field can be enhanced greatly. Recently, the huge Raman enhancement factor of $10^{13}-10^{15}$ in the "hot spots" was reported[2,3]. The huge enhancement factor of the "hot spots" made it responsible for the sensitivity of SERS detection. However, the Raman scattering cross section is given by the population-averaged far-field intensity contributed from the entire metallic structure surface. So a site like a touching point of two metal particles may not be dominant and such a metallic model cannot afford sufficient sensitivity of SERS detection in many cases. Therefore, design of the sample cell that could provide more "hot spots" is at the core of enhancing the sensitivity of SERS detection.

The strong electric field gradient arising from the attenuation of evanescent wave in nanometer can alter the Raman spectrum, which is called gradient-field Raman (GFR)[4]. GFR made some vibration modes not appear in the far-field Raman spectrum but appear in the near-field Raman spectrum, and the more vibration modes made the selection rules of the near-field Raman spectrum different from those of the far-field Raman spectrum. Therefore, it must provide more information on the characteristics of the sample in the nanometer scale.

There are several methods for numerical solving electromagnetic problems for any arbitrary geometry, such as Green's function method[5], multiple multipole (MMP) technique[6], and finite difference time domain (FDTD) technique[7], all of which have been applied to solve near-field optical problems. The FDTD technique has proved to be very flexible[8−15]. In this paper, the FDTD approach is used to design the sample cell in near-field SERS.

FDTD is a flexible numerical means of solving electromagnetic problems by integrating Maxwell's differential equations for an arbitrary geometry in three-dimensional space. The space is divided into small cubes called Yee cells[16], whose size is 1 nm in our case because of the computational limitation. The Mur's absorbing boundary condition is used at the sides of the simulated space.

Previous FDTD formulations were not capable of analyzing metals in that the negative permittivity of a metal can cause terms in FDTD expressions to become singular. Recent advances have extended the use of FDTD to the treatment of materials with frequency dependent, complex dielectric constants[17].

In this paper the metal is assumed to follow the Drude model. We can derive the permittivity by[18]

$$\varepsilon(\omega)=\varepsilon_0\left(1+\frac{\omega_{\rm p}^2}{\omega(j\nu_{\rm c}-\omega)}\right)=\varepsilon_0(1+\chi(\omega)), \qquad (1)$$

where $\nu_{\rm c}$ is the collision frequency, $\omega_{\rm p}$ the plasma frequency in radians, χ the susceptibility, and $j=\sqrt{-1}$. The optical constants of Ag used is $\varepsilon=-18.8+0.4j$ which is available in Ref. [19].

When the particle size is smaller than the mean free path of the conduction electrons (52 nm for silver), the magnitude of the real $\varepsilon'(\omega)$ and imaginary parts $\varepsilon''(\omega)$ of the dielectric function of the particle is affected by size. Considering the size effect and based on the Drude model, the size-dependent dielectric functions can be computed with[20]

$$\varepsilon'(\omega,r)=\varepsilon'_{\rm bulk}+\frac{\omega_{\rm p}^2}{\omega^2+\omega_{\rm d}^2}-\frac{\omega_{\rm p}^2}{\omega^2+\omega_{\rm r}^2}, \qquad (2)$$

$$\varepsilon''(\omega,r)=\varepsilon''_{\rm bulk}+\frac{i\omega_{\rm p}^2\varpi_{\rm r}}{\omega(\omega^2+\omega_{\rm r}^2)}-\frac{i\omega_{\rm p}^2\omega_{\rm d}}{\omega(\omega^2+\omega_{\rm d}^2)}, \qquad (3)$$

where ω, $\omega_{\rm p}$, and $\omega_{\rm d}$ are the light frequency, the plasmon frequency, and the bulk metal damping constant, respectively. Assuming that the metal particle-damping constant $\omega_{\rm r}$ is increased because of additional collisions with the boundary of the particle[21], $\omega_{\rm r}$ can be calculated by

$$\omega_{\rm r}=\omega_{\rm d}+B\frac{v_{\rm F}}{r}, \qquad (4)$$

where v_F is the electron velocity at the Fermi level (1.39×10^6 m/s) and B is the theory dependent quantity of order 1.

In the first case, the field intensity distributions of bi-spherical Ag particles under the excitation of plane wave and evanescent wave are simulated. Figures 1(a) and (b) show the electric field intensity distribution of transverse and longitudinal bi-spherical Ag particles placed on the glass substrate under the excitation of evanescent wave. The evanescent wave is formed by the total internal reflection of 632.8-nm plane wave at the interface of glass and air. Figure 1(c) is for the case of transverse bi-spherical Ag particles under the excitation of 632.8-nm plane wave. The diameters of Ag particles are all 30 nm. All images in this paper display the intensity enhancement in the plane crossing centers of two particles and parallel to the xoz plane.

As shown in Fig. 1, "hot spots" are all confined within a few nanometers around the touching point of two particles and distribute as a circle, which can be explained at the basis of localization of the local surface plasmon (LSP) field at the edge. Comparing Fig. 1(a) with Fig. 1(b), we can see that the strong gradient arising from the attenuation of evanescent wave in z direction contributes to the electric field enhancement. Note that much larger electric field intensity enhancement factor of $10^5 - 10^6$ is got for these three cases, in which the greatest is for the case of Fig. 1(b).

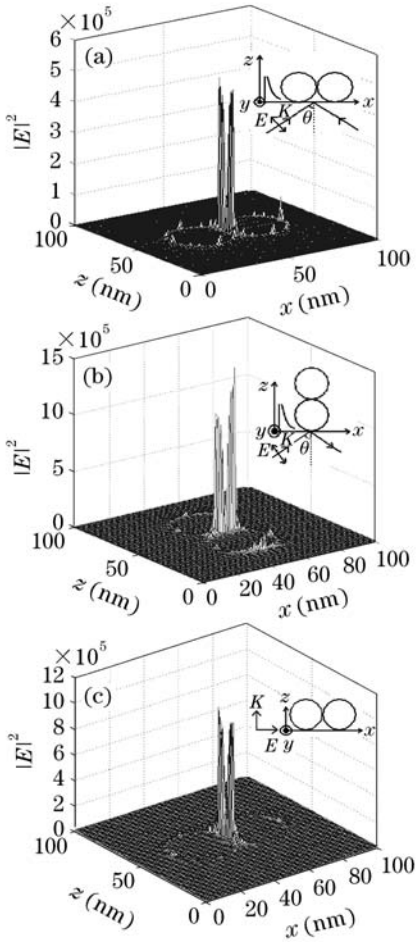

Fig. 1. FDTD simulated electric field intensity distribution for bi-spherical Ag particles with diameter of 30 nm. (a) Transverse array under the excitation of evanescent wave formed by the total internal reflection of 632.8-nm plane wave at the interface of glass and air, incident angle is 55°; (b) longitudinal array under the excitation of evanescent wave; (c) transverse array under the excitation of 632.8-nm plane wave. The amplitude of the plane wave is 1 V/m and the polarization of excitation is indicated in the figure.

However, the Raman scattering cross section is given by the population-averaged far-field intensity contributed from the entire Ag particles surface, so a site like a touching point of two metal particles may not be dominant and such a metal model cannot afford sufficient sensitivity for the SERS detecting in many cases. So design of the sample cell that can provide not only huge electric field intensity enhancement in "hot spots" but also many "hot spot" are needed to enhance the sensitivity of SERS detection further.

In order to obtain a model which could produce more "hot spots" but not single "hot spot", a sample cell which is arranged according to Fig. 2 was designed. In this model, the configuration of Ag film-Ag particles with no gap size is adopted in order to produce equivalent field intensity enhancement, for the Ag flat substrate surface is island film actually when the film is very thin. Under this condition, the electric field intensity distributions for this configuration illuminated by evanescent wave and plane wave are simulated.

As can be seen in Fig. 2, the local field intensity enhancement of $10^5 - 10^6$ is obtained under two kinds of excitation. What we should pay attention to is that additional "hot spots" appear around centers between Ag particles and Ag thin flat substrate. The massive field intensity enhancement is also produced in these "hot spots", which can improve the sensitivity of SERS

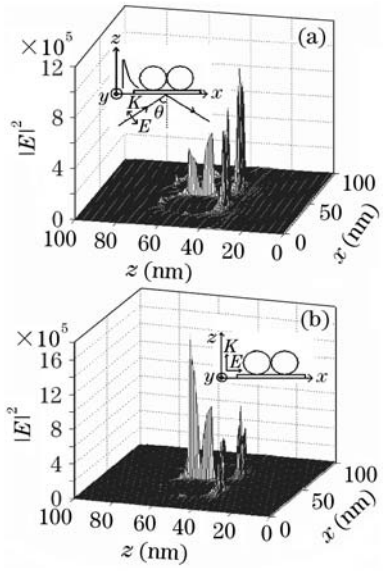

Fig. 2. FDTD simulated electric field intensity distribution for bi-spherical Ag particles placed above the Ag flat substrate with thickness of 5 nm. (a) Transverse array under the excitation of evanescent wave; (b) transverse array under the excitation of 632.8-nm plane wave. The amplitude of the plane wave is 1 V/m and the polarization of excitation is indicated in the figure.

detection. For the excitation of evanescent wave shown in Fig 2(a), field intensity enhancement of "hot spots" around centers between Ag particles and Ag flat substrate is greater than that of "hot spots" around the touching point of two particles. The condition is contrary for the excitation of plane wave shown in Fig. 2(b). The Ag thin flat substrate must assure that the incident wave can penetrate through it, so the adoptive thickness of the Ag flat substrate in this configuration is 5 nm.

On the basis of numerical solutions above, we hold two Ag flat substrates with thickness of 5 and 50 nm down and up bi-spherical particles to form the sample cell. As shown in Fig. 3, more "hot spots" appear around centers between Ag particles and above Ag film for two kinds of excitation by comparing with Fig. 2. On the other hand, the upper Ag film can press Ag particles to array transversely to produce great enhancement under the excitation of plane wave whose polarization is shown in Fig. 3(b). Furthermore, the upper Ag film can limit the scattering light into the configuration to interact with Ag particles many times, which also may enhance the scattering field. Similar to Fig. 2, the field intensity enhancement of "hot spots" around centers between Ag films and Ag particles is greater than that of "hot spots" around the touching point of two Ag particles for the excitation of evanescent wave and the case is contrary for the excitation of plane wave.

From the numerical simulations above, we could see that the experimental scheme following the configuration shown in Fig. 3 has better sensitivity of SERS detection than the one following Figs. 1 and 2. Therefore, the experimental scheme for better SERS detection was put up, as shown in Fig. 4.

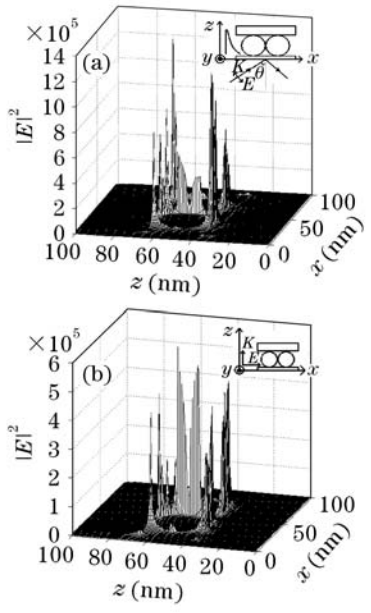

Fig. 3. FDTD simulated electric field intensity distribution for bi-spherical Ag particles placed between two Ag flat substrates with thicknesses of 5 nm below one and 50 nm above one. (a) Transverse array under the excitation of evanescent wave; (b) transverse array under the excitation of 632.8-nm plane wave. The amplitude of the plane wave is 1 V/m and the polarization of excitation is indicated in the figure.

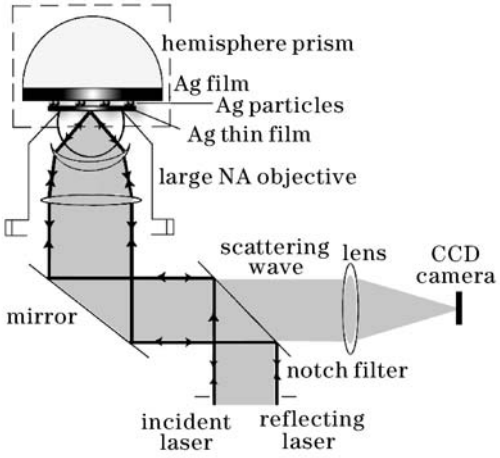

Fig. 4. Schematic of near-field SERS microscopy. The portion surrounded by the dashed line is the sample cell in which the sample is placed and detected.

For the near-field SERS experiments, we employ an optical illumination system consisting of a high numerical aperture (NA) objective lens and an annular illumination, as shown in Fig. 4[22]. Both the transmitted light (NA < 1) and the evanescent field formed by the objective lens (NA $= 1.65$) can irradiate the sample in this configuration. Under the illumination of this instrument, many "hot spots" may be produced to improve the sensitivity of SERS detection. The other merit of the sample cell is that the increased output of the excitation owing to the large NA objective lens, which also can enhance the Raman signal. And new Raman spectrum may come forth because of GFR of evanescent wave.

The interference of the incident light in this instrument must be considered. Otherwise, the counteraction of polarization in a certain direction may reduce the field intensity enhancement. So we must add a slice which can alter the phase of the partial incident light to ensure enhancing the Raman signal in the greatest degree.

The use of the Ag nanometer structure as a strong enhanced, localized excitation source can improve the sensitivity of the Raman microscopy. The high electric field enhancement is calculated for the configuration of Ag film-Ag particles under the excitation of plane wave and evanescent wave in this pursuit. In the case of two adjoining Ag nanoparticles, the electric field enhancement volume is constrained around the contact point between two particles. And the enhancement intensity can be as high as 10^6 when the orientation of the incident polarization is parallel to the dimmer line. However, for the case of Ag film-Ag particles, more "hot spots" come forth around centers between Ag particles and Ag films under two kinds of excitation. The intensity enhancement of additional "hot spots" is comparable with that of "hot spots" around the touching point between two Ag particles.

The sample cell can not only produce more "hot spots" but also increase the output of excitation owing to the large NA, which all may improve the sensitivity of SERS detection. Moreover, new spectrum may be generated because of GFR of evanescent wave to provide more nanometer information of the sample. The interference of the incident light must be considered to ensure the

greatest field intensity enhancement.

S. Wu is author to whom the correspondence should be addressed, his e-mail address is wsf@dlut.edu.cn.

References

1. M. Moskovits, Rev. Mod. Phys. **57,** 783 (1985).
2. K. Kneipp, Y. Wang, H. Kneipp, L. T. Perelman, I. Itzkan, R. R. Dasari, and M. S. Feld, Phys. Rev. Lett. **78,** 1667 (1997).
3. H. Xu, E. J. Bjerneld, M. Käll, and L. Börjesson, Phys. Rev. Lett. **83,** 4357 (1999).
4. E. J. Ayars, H. D. Hallen, and C. L. Jahncke, Phys. Rev. Lett. **85,** 4180 (2000).
5. O. J. F. Martin, C. Girard, and A. Dereux, Phys. Rev. Lett. **74,** 526 (1995).
6. C. Hafner, *The Generalized Multiple Multipole Technique for Computational Electromagnetics* (Artech, Boston, 1990).
7. A. Taflove and M. E. Brodwin, IEEE Trans. Microwave Theory and Tech. **23,** 623 (1975).
8. R. X. Bian, R. C. Dunn, X. S. Xie, and P. T. Leung, Phys. Rev. Lett. **75,** 4772 (1995).
9. D. A. Christensen, Ultramicroscopy **57,** 189 (1995).
10. J. L. Kann, T. D. Milster, F. Froehlich, R. W. Ziolkowski, and J. Judkins, Ultramicroscopy **57,** 251 (1995).
11. H. Nakamura, T. Sato, H. Kambe, K. Sawada, and T. Saiki, J. Microscopy **202,** 50 (2001).
12. R. G. Milner and D. Richards, J. Microscopy **202,** 66 (2001).
13. B. B. Akhremitchev, S. Pollack, and G. C. Walker, Langmuir **17,** 2774 (2001).
14. H. Furukawa and S. Kawata, Opt. Commun. **148,** 221 (1998).
15. J. T. Krug II, E. J. Sa'nchez, and X. S. Xie, J. Chem. Phys. **116,** 10895 (2002).
16. K. S. Yee, IEEE Trans. Ant. Propagat. **14,** 302 (1966).
17. R. J. Luebbers, F. Hunsberger, and K. S. Kunz, IEEE Trans. Ant. Propagat. **39,** 29 (1991).
18. L. D. Landau and E. M. Lifshitz, *Electrodynamics of Continuous Media* (Elmsford, New York, 1984).
19. P. B. Johnson and R. W. Christy, Phys. Rev. B **6,** 4370 (1972).
20. U. Kreibing and M. Vollmer, *Optical Properties of Metal Clusters* (Springer, Berlin, 1995).
21. C. F. Bohren and D. R. Huffman, *Absorption and Scattering of Light by Small Particles* (Wiley, New York, 1998).
22. S. Wu and G. Wu, *Near-field enhanced Raman scattering sample cell using evanescent wave for both excitation and reception* (in Chinese) Chinese Patent, the Application Number of Inventing 021544689 (2003).